

# Using high resolution satellite imagery in vulnerability modeling: an object-oriented approach

E. Nolte <sup>a</sup> and F. Wenzel <sup>b</sup>

<sup>a</sup> University of Karlsruhe, Hertz Str. 16, Karlsruhe, Germany;

<sup>b</sup> University of Karlsruhe, Hertz Str. 16, Karlsruhe, Germany

## ABSTRACT

The May 2006 Central Java earthquake ( $M_w$  6,3) heavily struck the Special Province of Yogyakarta, Indonesia. The widespread damage and high number of casualties revealed the necessity of vulnerability assessment within this region. A vulnerability and risk analysis was conducted using a GIS-based Indicator - Index Method. In this analysis very high resolution satellite images were used for two purposes: Firstly to validate the risk map by detecting damaged areas. This led to the development of an object-based and a pixel-based methodology for damage detection. The detected damage areas were analyzed on a building unit scale. For each building unit the damage was calculated. Secondly to extract detailed information on the spatial distribution of landuse in the study area. This was conducted using an object-based, multiresolution approach.

**Keywords:** Yogyakarta, object-oriented image analysis, image classification, vulnerability, risk, indicators

## 1. INTRODUCTION

Remotely sensed images from satellites have become an important tool to assess vulnerability of urban and rural areas. The main interest is related to the assessment of building vulnerability and damage. About 75 % of fatalities attributable to earthquakes are due to the collapse buildings.<sup>1</sup> But visual interpretation is time-consuming and labor-intensive, so fast and efficient techniques for a identification of building damage distribution are needed. For vulnerability analysis the utilization of GeoInformation Technology arises directly from the capabilities of this technology in generating data at scale of interest and allowing for spatial analysis. This has a special relevance for working with data from developing countries where availability of information is often limited.

## 2. CASE STUDY

The study area is located in the Regency of Bantul within the Special Region of Yogyakarta, Island of Java, Indonesia (see Fig.1). The tectonics of Java are dominated by the subduction of the Australia plate north-northeastward beneath the Sunda plate with a relative velocity of 6 to 15 cm/year.<sup>2,3</sup> In May 2006 an earthquake with a magnitude of 6,3 on the Richter scale struck the district of Yogyakarta City and its neighboring districts at 05:53:58 AM local time \*. The widespread damage and high number of casualties revealed the necessity of vulnerability assessment within this region. Along a 30 km stretch of the Opak River Fault (district Bantul), the 26 May earthquake caused severe damage to the densely populated area, leaving about 6.200 dead, 38.000 injured and over 1.500.000 displaced<sup>4</sup> (see Fig.1).

The satellite data utilized in the remote sensing analysis are orthorectified Quickbird images acquired on 11.07.2003 and 31.05.2006 with a panchromatic resolution of 0,60 m and a multispectral resolution of 2,4m.

---

Further author information: (Send correspondence to Eike Nolte)

E. Nolte: E-mail: Eike.Nolte@gpi.uni-karlsruhe.de, Telephone: 0049 0721 6084507

\*USGS,<http://earthquake.usgs.gov/eqcenter/recenteqsww/Quakes/usneb6.php>)

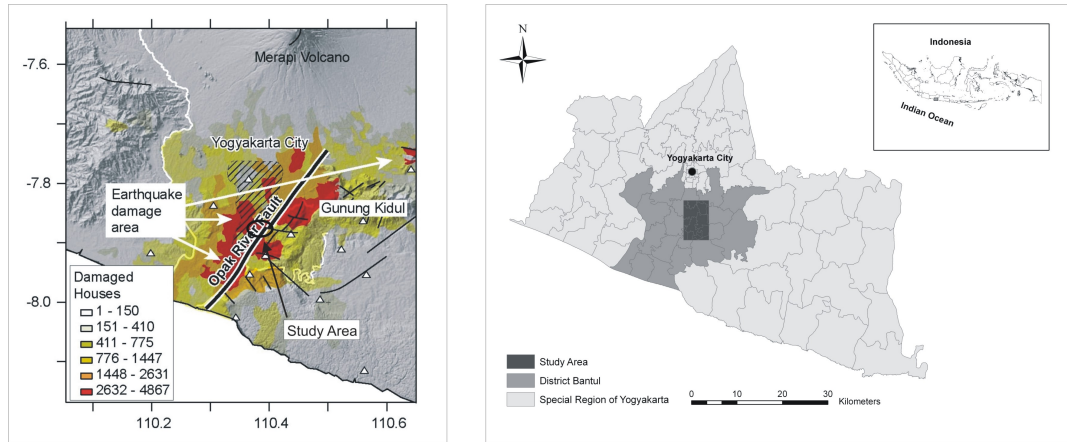


Figure 1. (Left) Earthquake damage area south of Yogyakarta City (dashed area). The most severe damage is concentrated along the Opak River Fault. The earthquake area is illustrated by the number of destroyed and heavily damaged houses.<sup>5</sup> (Right) Location of the study area within the Special Region of Yogyakarta.

### 3. RISK MODELING USING GIS TECHNOLOGY

The risk analysis was carried out using a step - wise indicator development approach including an three - tier Index Method<sup>6</sup> to implement the hazard - specific weights into the analysis. The modeling procedure encompasses a susceptibility or hazard model, a vulnerability model and a risk model. In terms of hazards and vulnerability, risk is represented by the following mathematical expression:<sup>7</sup> Risk = Vulnerability × Hazard.

The formulation of goals serve as starting point to identify the relevant factors and indicators.<sup>8</sup> In this analysis the primary goal was to reveal the vulnerability of communities potentially effected by earthquakes within the study area.

#### 3.1 Step - Wise Indicator Development Approach

The very complexity of the concept of vulnerability requires a reduction of potentially available data to a set of important indicators and criteria that facilitate an estimation of vulnerability.<sup>8</sup> Four relevant physical factors that contribute to earthquake risk were determined: climate, topography, geology and environment. For each of these factors representative indicators were developed (see Table .1). For the susceptibility analysis a hazard specific weight is applied to the previously defined indicators, because indicators have different meanings for specific hazards.<sup>9</sup>

Table 1. Factors, representative indicators and assigned indices ( $I_2, I_3, I_{Total}$ ). The indices were assigned relative to the indicator's impact on earthquake risk.

Factor	Indicators	Index $I_2$	Index $I_3$	Index $I_{Total}$
Geology	Lithology	1,0	0,4	0,40
Environment	Soil	0,6	0,3	0,18
	Erosion	0,2		0,06
	Geomorphology	0,2		0,06
Topography	Slope	0,5	0,2	0,10
	Exposition	0,1		0,02
	Curvature	0,2		0,04
	Elevation	0,2		0,04
Climate	Temperature	0,3	0,1	0,03
	Precipitation	0,7		0,07
		$\sum_{Factor} = 1$	$\sum = 1$	$\sum = 1$

For the susceptibility analysis a hazard specific weight is applied to the previously defined indicators, because indicators have different meanings for specific hazards.<sup>9</sup> First, each indicator was classified and every class was weighted ( $I_1$ ) individually according to its importance for the specific indicator. In the next step, the indicators were weighted ( $I_2$ ) according to their importance for the factor they represent. The third index  $I_3$  was assigned by weighting the factors relative to each other. The total index  $I_{Total}$  was calculated by the multiplication of index  $I_2$  and index  $I_3$ . All applied indices range from 0 (zero) to 1 (one). Finally, the susceptibility is calculated by multiplying the Index  $I_{Total}$  with the Indicator. For each cell of the study area the susceptibility is given by the sum of the susceptibility of all indicators. The hazard map shows that the areas with the highest susceptibility are mainly located in the northwest of the study area. The widespread, soft sediments of the Yogyakarta and the Sleman Formation and the supposed amplification of the ground motion during the May 2006 earthquake lead to the higher hazard values in contrast to the stable, limestone formation in the southeast.<sup>5</sup> The increased susceptibility along the major rivers and channels can be correlated with the erosion due to accumulated water flow carrying woods and other materials.

### 3.2 Vulnerability and Risk Analysis

The vulnerability of an area depends on its exposure. There were only few data available on the inventory of the study area, thus only physical infrastructure e.g. street network and landuse as well as population density as a social indicator could be considered. Each element was weighted according to its specific importance to the vulnerability e.g. hospitals were assigned a higher index than touristic sights. In the last step the risk was calculated using the following equation:<sup>7</sup>  $Risk = Vulnerability \times Hazard$ . The results were display as maps to allow a first overview (see Fig.2).

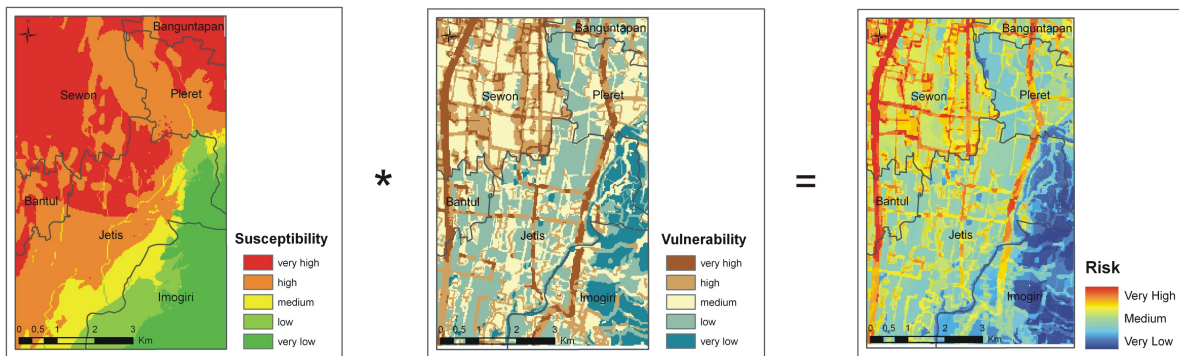


Figure 2. Schema for calculation the risk map using the susceptibility and vulnerability layer.

## 4. OBJECT ORIENTED IMAGE ANALYSIS

Object orientated image analysis is based on the human image understanding. The human perception includes not only grey values but also pattern, shape and homogeneity heterogeneity respectively. The software package Definiens Developer 7 was used for the image analysis because of its wide range of object orientated image analysis tools. In this study satellite images were used for two different purposes: to improve the landuse dataset and to extract information of the damage distribution. For the latter, two approaches were analyzed: a object-oriented and a multi-temporal, pixel-based approach. For the landuse classification only a mono-temporal, object-oriented image analysis was conducted.

### 4.1 Image Segmentation

For the mono-temporal, object-oriented approach the software package Definiens Developer 7 was used. The first step was to segment the image into meaningful image objects. There are two segmentation principles: Top-down and bottom-up segmentation.<sup>10</sup> The top-down segmentation means cutting objects into smaller objects. The bottom-up segmentation assembles objects to create larger objects. There are several bottom-Up segmentation

algorithms within Definiens Developer 7. One of the most widely used is the multiresolution segmentation algorithm. It is based on a pairwise region merge technique.<sup>11</sup> As a merging algorithm Definiens uses the local mutual best fitting algorithm. The merging decision is based on local homogeneity criteria describing the similarity of image objects. The maximum standard deviation of the homogeneity criteria in regard to the weighted image layers is defined using the so called scaleparameter (s. Fig. 3). Four internal criteria are used to control the scaleparameter: compactness, smoothness, color and shape.<sup>12</sup> Each sub-criteria can be adjusted by the user, thus the merging procedure and the size of the image objects can be optimized for specific purposes. The in percent assigned weights are equalized to the value of 1. The balance at which these criteria are applied depends on the desired output.<sup>13</sup>

$$f = w \cdot h_{Color} + (1 - w) \cdot h_{Shape} \tag{1}$$

with  $h_{Color}$  being the color criterion,  $h_{Shape}$  being the shape criterion and  $w$  being the user defined weight with  $0 = w = 1$

### 4.2 Classification

Here, classification is understood as the procedure to associate an image object with an appropriate class. Each class is characterized by specific features contained in its class description. In this study a fuzzy logic classification was used, because it allows pixels or image objects to have membership in more than one class and therefore better represent the imprecise nature of the data.<sup>14</sup>

### 4.3 Debris Detection

For the debris detection the image acquired on 31 May 2006 was used. First, all non-residential and clouded residential areas were masked out using a vector layer. For the segmentation four multispectral (R,G,B,NIR) and one panchromatic band was used. A very low scaleparameter was used, because of the heterogeneity of the buildings (Scaleparameter 15, Shape 0,3, Compactness 0,9).



Figure 3. Segmentation and classification applied on multispectral Quickbird satellite images. In the left picture a image object was segmented using a scale parameter of 15 (red square), in the right picture the image object was classified as a red house.

For the classification the following classes were defined: dark houses, red houses, red houses in shadow, blue houses, white houses, debris and vegetation in residential areas. For each class a set of suitable feature was selected. Each membership is defined using fuzzy logic functions. The single feature are connected by fuzzy operators in order to combine the different membership degrees to a single membership value. Besides the features provided by Definiens, customized features such as the NDVI (Normalized Differenced Vegetation Index) and features that calculate the percentage of each band for the brightness were developed. The following features were used for the debris class description: NDVI, Blueness, Brightness and not classified as red houses. The Brightness and Blueness were calculated following<sup>15,16</sup> For the membership functions of each feature and the selected value ranges see Appendix A. The detected damage areas compass damage of grade 4 and 5 i.e. very heavy damage and complete destruction,<sup>17,18</sup> A total damage area of 0,61 km<sup>2</sup> was detected. The distribution of the damage was used to evaluated the risk map. In the sub-district of Sewon the extracted damage areas correlated well with the areas of high to medium risk. In Imogiri (south-southeastern part of the studyarea) the damage areas were concentrated around the main roads. This is mainly due to the generalizing assumption that the population density is equally distributed. A more realistic picture is a concentration of the population along the main roads.

For the pixel-based approach the software package PCI Geomatica was used. For each band (R,G,B) the images acquired 2003 and 2006 were divided using the image rationing method. Changes were detected with a user-defined threshold for mean and standard deviation. Ideally, no change should result in a pixel value equal to 1. For the blue band 0,63 km<sup>2</sup>, for the red band 0,61 km<sup>2</sup> and for the green band 0,64 km<sup>2</sup> of damage area was detected. Because of the minor differences one band was selected as a representative and used in the comparison with the results of the object-oriented approach. In the following the results of the object-oriented debris detection will be compared with the results from the pixel-based approach.

#### 4.4 Analysis of damage distribution

The results of the damage detection was analyzed using the house distribution within a selected areal of 29662,88 m<sup>2</sup> (subdistrict Sewon). All houses were digitized using the panchromatic image from 2003. In case that single houses could not be registered, building units were used instead. This was necessary due to the lack of land register data. The houses cover 33,5 % of the areal. First, the results from the object-based approach were analyzed. Assuming an equally distributed damage within the areal, 31,6 % of the houses were destroyed or heavily damaged. The results for the pixel-based method show that 15,43 % of the houses were destroyed. Assuming an equally distributed damage, the object-oriented detected area is twice as large as the pixel-based detected area. In order to give a more realistic picture, the damage distribution per building unit was calculated. On the building level scale, the percentage of damage show the same trend. Building units with a high percentage of damage were identified as such with both approaches (see Fig.4).

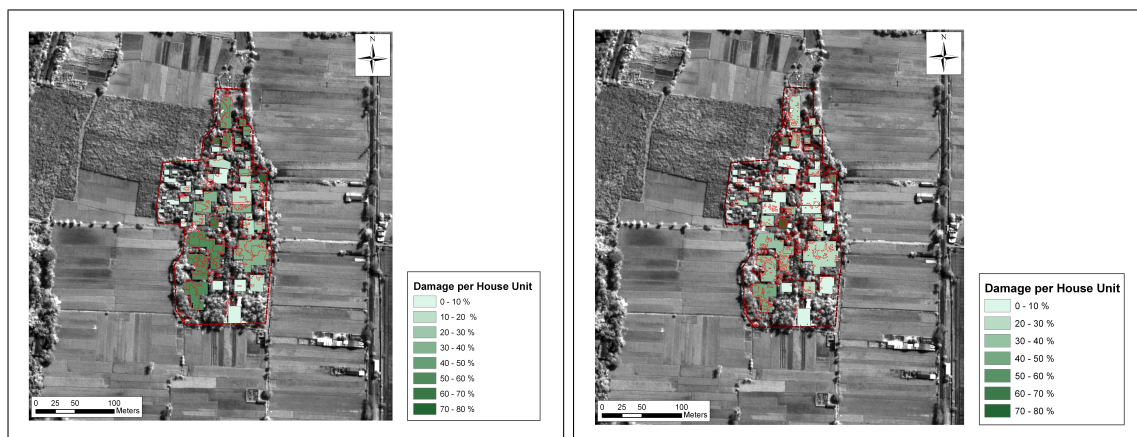


Figure 4. Damage per building unit for a small test areal. The left picture displays the results of the object-oriented approach, the right picture of the pixel-based approach.

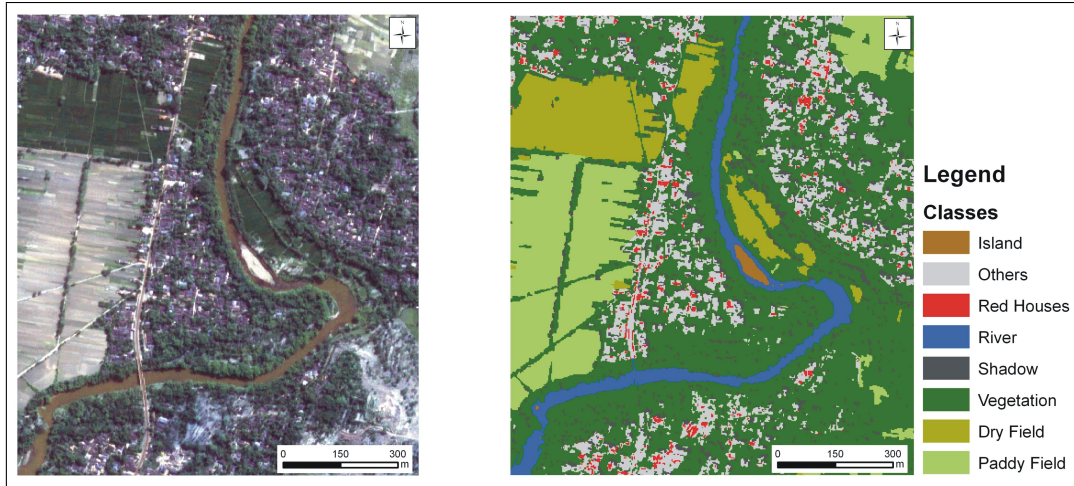


Figure 5. (Right) Multispectral Quickbird image with 2,4 m resolution. (Left) Results of the land use classification.

#### 4.5 Landuse Classification

For the landuse extraction a multiresolution segmentation was conducted. A very small scaleparameter of 15 was used to segment shadows and the water areas. After classifying the small segments, the scale parameter was iteratively increased for the remaining non-residential areas. Finally, the scale parameter generating the most meaningful image objects was chosen for the classification (scaleparameter 80, shape 0,3, compactness 0,7). For the membership functions for all classes used for the landuse classification see Appendix A. In contrast to the debris classification, not only spectral image object features were used in the landuse analysis but also shape, relational and textural features. The results for the landuse classification are displayed in Fig.5.

### 5. RESULTS

In this section the results of the Risk Analysis and the image analysis will be presented. The risk assessment revealed the unequal distribution of risk within the study area. The overlap of unfavorable, geological conditions with high population density and important access roads lead to a significant higher risk in the northwest (Sewon). In the southeast the lower population density and the hard bedrock dominated underground results in a lower risk. It is important to point out that the generalized assumptions on population distribution and other feature sometimes lead to a misinterpretation of the circumstances. For example, using an equal distribution of population lead to a low risk than the damage distribution revealed afterwards. The analysis of the debris distribution and the calculated risk map showed satisfying correlation. Also the pixel-based and the object-oriented approach did numerically detect nearly the extent of damaged areas for the study area, on a smaller scale the considerable difference became obvious. But the results show still the same trend on the building unit scale.

The results of the image classification for landuse detection are displayed in Fig 5. The classifications stability (Fig.6) indicates that the smaller segments are less stable than the larger segments. Especially the mixed vegetation segments show unstable classification because the membership value of the second best classification result is very similar to the best result. Further accuracy assessment is still to be conducted. There were no reference data available, therefore they will be generated using the panchromatic image of 2003. A object-oriented accuracy assessment will be carried out using GIS software. Furthermore, the impact of the improved landuse data on the GIS-model is yet to be analyzed.

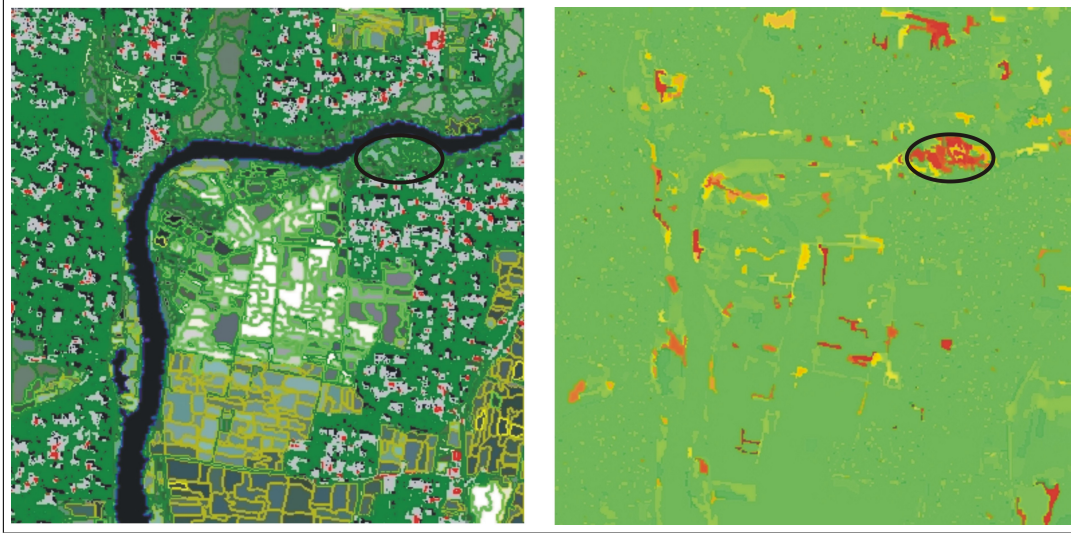


Figure 6. (Right) Segmentation results for multiresolution approach. (Left) Classification stability: The smaller segments show lower classification stability (red segments).

## 6. CONCLUSION

In this paper the results of vulnerability analysis using a GIS-based Indicator - Index Method were presented. The application of very high resolution satellite images for validation risk maps was analyzed. Furthermore, the improvement possibilities of landuse data using Quickbird image were tested. Also the GIS data were scarce, the generated map give a good picture of the general risk distribution. The satellite images used are only partially suitable for debris detection because of their limited number of bands. But for landuse detection using a object-oriented approach the image proved to be suitable.

## APPENDIX A. TABLES

Table 2. Features for class debris and developed membership functions

Feature	Membership Function Type	Value Range
NDVI	smaller than	0,20 - 0,31
Blueness	smaller than	80,61 - 93,00
Ivits Brightness	approximate Gaussian	500,00 - 900,00
not classified as red houses	larger than	0,00 - 0,10

Table 3. Classes used for landuse classification, class description and membership functions. For the landuse classification not only spectral features but also textural and shape feature were applied.

Class	feature	Membership Function	Value Range
Water	Mean Layer 4	smaller than	100,00 - 230,00
	NDVI	smaller than	-0,30 - 0,45
River	Area	larger than	400 m <sup>2</sup>
Paddy Field	Maximum Difference	smaller than	0,20 - 1,20
	Saturation HSI	smaller than	0,20 - 0,80
Dry Field	Mean Layer 4	larger than	300 - 600
	NDVI	larger than	0,20 - 0,74
Vegetation mix	GLCM Homogeneity (all dir.)	smaller than	0,55 - 0,70
Residential Area	not Non-Residential Area	-	-
Shadow in Residential Area	Brightness	smaller than	170,00 - 195,00
Red Houses	Redness	larger than	28,50 - 30,00
	Greenness	larger than	29,00 - 32,00

## REFERENCES

- [1] Weston, A.-J., Burton, P., and Lovett, A., [*Imagery and Ground Truth in an assessment of the Built Environment with an Earthquake Impact Scenario*] (2003).
- [2] Stüben, D. and Neumann, T., [*Erschließung und Bewirtschaftung unterirdischer Karstfließgewässer in Mitteljava, Indonesien (Förderkennzeichen 02WT0428) Teilprojekt 2: Wasser/Gestein-Wechselwirkungen in den Karstgebieten von Wonosari: Verwitterungsresistenz der Kalkgesteine, Wasserwegsamkeiten im Gesteinsverbund und Verbesserung der Wasserqualität*] (September 2006).
- [3] Brüstle, W., Renault, P., Schlüter, F.-H., and Swain, T., [*Erdbebenschäden bei Yogyakarta, Indonesien*], DGE (2007).
- [4] Walter, T., Luehr, B.-G., Wang, R., Sobiesiak, M., Günther, E., Grosser, H., Wetzel, H.-U., Milkereit, C. and Zschau, J., Wassermann, J., Behr, Y., Harjadi, P., and Brotopuspito, K., “A city built on sand: First results of the earthquake-task-force in the disaster area of the 26 may 2006 yogyakarta earthquake,” (2006).
- [5] Walter, T. , Wang, R., Luehr, B.-G., Wassermann, J., Behr, Y., Parolai, S., Anggraini, A., Günther, E., Sobiesiak, M., Grosser, H., Wetzel, H.-U., Milkereit, C., Sri Brotopuspito, P., Harjadi, P., and Zschau, J., “The may 2006 magnitude 6.4 yogyakarta earthquake south of mt. merapi volcano: Did lahar deposits amplify ground shaking and thus lead to the disaster ?,” *Geochem. Geophys. Geosyst.* **9** (2008).
- [6] Juang, C., Lee, D., and Scheu, C., “Mapping slope failure potential using fuzzy sets,” *Journal of Geotechnical Engineering* **118**, 475 – 494 (1992).
- [7] UN/ISDR, [*Living with Risk: A Global Review of Disaster Reduction Initiatives*], UN Publications, Geneva (2004).
- [8] Birkmann, J., “Indicators and criteria for measuring vulnerability: Theoretical bases and requirements,” in [*Measuring Vulnerability to Natural Hazards: Towards a disaster resilient society*], Birkmann, J., ed., United Nation University Press (2006).
- [9] Bollin, C. and Hidayat, R., “Community-based disaster risk index,” in [*Measuring Vulnerability to Natural Hazards*], Birkmann, J., ed., United Nation University Press (2006).
- [10] Definiens AG, München, *Definiens Developer 7 Userguide* (2007).
- [11] Baatz, M. and Schäpe, A., “Multiresolution segmentation: an optimization approach for high quality multi-scale image segmentation,” *AGIT-Symposium Salzburg* , 12–23 (2000).
- [12] DefiniensAG, [*Definies Developer 7 Reference Book*], DefiniensAG (2007).
- [13] Thomas, N., Hendrix, C., and Congalton, R., “A comparison of urban mapping methods using high-resolution digital imagery,” *Photogrammetric Engineering and Remote Sensing* **69**, 963 – 972 (2003).
- [14] Shackelford, A. and Davis, C., “A hierarchical fuzzy classification approach for high-resolution multispectral data over urban areas,” *IEEE Transactions on geoscience and remote sensing* **41**, 1920–1932 (2003).
- [15] Kauth, R. and Thomas, G., “The tasseled cap - a graphic description of the spectral-temporal development of agricultural crops as seen by landsat,” in [*Proceedings of the Symposium of Machine Processing of Remotely Sensed Data*], 41 – 51, Prudue University (July 1976).
- [16] Ivits, E., “Tasseled cap parameters for ikonos,” tech. rep., Abteilung Fernerkundung und Landschaftsinformationssysteme, Universität Freiburg (2005).
- [17] Grünthal, G., [*European Macroseismic Scale*], vol. 15, Luxembourg : Centre Européen de Géodynamique et de Séismologie (1998).
- [18] Bitelli, G., Camassi, R., Gusella, L., and Mognol, A., “Image change detection on urban area: the earthquake case,” (2004).